CFD-Based Investigation of Flow Through an Orifice Plate Meter under Different Conditions

Esam Hamza [1*], Ahmed Khalifa [2], Anas Geri [3], Nasreddin Al-Zalitani [4],
Abdulgader Alsharif [5] , Hamza Aagela[6]
[1, 2, 3, 4] Department of Mechanical and Industrial Engineering, Faculty of Engineering, University of Tripoli, Tripoli, Libya
[5] Department of Electrical and Electronic Engineering, College of Technical Sciences, Sebha, Libya
[6]Department of Engineering, School of Computing and Engineering, University of Huddersfield, Huddersfield, United Kingdom
*Corresponding author: es.hamza@uot.edu.ly

تحقيق مبني على ديناميكيات الموائع الحسابية للتدفق عبر مقياس ذو الفتحة في ظل ظروف مختلفة

عصام محمد حمزة[1*]، أحمد عبد الحكيم خليفة[2]، أنس ساسي جري[3]، نصرالدين نوري الزليطني[4]
عبد القادر حسين الشريف[5]، حمزة عقيلة[6]
[4،3،2،1] قسم الهندسة الميكانيكية والصناعية، كلية الهندسة، جامعة طرابلس، طرابلس، ليبيا
[5] قسم الهندسة الكهربائية الإلكترونية، كلية العلوم التقنية، سبها، ليبيا
[6] قسم الهندسة، مدرسة الحاسب والهندسة، جامعة هدرسفيلد، هدرسفيلد، المملكة المتحدة

Received: 03-04-2025; Accepted: 28-05-2025; Published: 08-06-2025

Abstract:
Orifice plate meters are widely used for flow rate measurement in pipelines but their accuracy can be significantly affected under turbulent flow conditions. This study investigates the performance of orifice plate meters under turbulent flow conditions using a two-dimensional Computational Fluid Dynamics (CFD) model. The influence of orifice beta ratio (the ratio of orifice diameter to pipe diameter), surface roughness, and fluid type (water, air, and oil) on the discharge coefficient (C_d) and pressure drop was analyzed through 45 simulations. Results show that increasing the beta ratio (0.42~0.58) increases the discharge coefficient (C_d) and reduces pressure drop for all fluids, improving flow efficiency. Surface roughness had negligible impact on (C_d) at Reynolds number = 50,000, while velocity profiles remained consistent across fluids, with maximum velocity decreasing at higher beta ratios. Vortex formation at the outlet diminished with increasing beta ratios and disappeared entirely at the highest beta ratio value. Velocity and pressure contours show the effects of these parameters on (C_d), illustrating the performance of orifice plate meters in turbulent flow scenarios.

Keywords: Orifice Meter, Computational Fluid Dynamics (CFD), Discharge Coefficient, Reynolds Number, Beta Value.

الملخص
تبحث هذه الدراسة في تأثر دقة أداء مقياس ذو الفتحة في ظل ظروف التدفق المضطرب على قياس معدل التدفق في خطوط الأنابيب باستخدام نموذج تحليل عددي لديناميكا الموائع ثنائي الأبعاد. تم تحليل تأثير نسبة بيتا (نسبة قطر الفتحة من قطر الأنبوب)، وخشونة السطح، ونوع المائع (ماء وهواء وزيت) على معامل التصريف (Cd) وانخفاض الضغط، من خلال إجراء 45 عملية محاكاة. تُظهر النتائج أن زيادة نسبة قطر الفتحة من قطر الأنبوب تزيد من معامل التصريف وتقلل من انخفاض الضغط لجميع الموائع ضمن الدراسة. مما يحسن من كفاءة التدفق. كان لخشونة السطح تأثير ضئيل على معامل التصريف عند يكون عدد رينولدز مساويا 50000. بقيت منحنيات السرعة متسقة عند كل الموائع، مع انخفاض السرعة القصوى عند نسب بيتا العليا. تضاءل تكوّن الدوامات عند المخرج مع زيادة نسب بيتا، واختفت تمامًا عند أعلى قيمة لنسبة بيتا. منحنيات السرعة والضغط أيضا تُظهر تأثيرات المتغيرات التي تم اعتبارها في الدراسة على قيمة (Cd)، مما يوضح أداء مقياس ذو الفتحة في سيناريوهات التدفق المضطرب.

الكلمات المفتاحية: مقياس ذو الفتحة، ديناميكيات الموائع الحسابية، معامل التصريف، رقم رينولدز، قيمة بيتا

Introduction

An orifice is a precisely designed opening in a plate, which is used for measuring, monitoring or controlling fluid flow rates, commonly employed in various industrial applications such as oil and gas, chemical processing, and water treatment. While its construction appears simple—consisting of a metal plate with an orifice at its center, positioned between flanges with pressure tapings located along the pipe walls—its design and construction is more intricate than it seems, and the flow behavior it produces is highly complex. Although the behavior of the orifice plate can be predicted, these predictions rely on experimental data. Typically, the inlet flow is turbulent as it approaches the orifice plate. An upstream pressure tapping, located one pipe diameter before the orifice plate, measures the static pressure at the pipe wall, see Figure 1. Near the plate, the flow converges toward the orifice, creating a recirculation vortex around the plate's outer edge. As the flow passes through the orifice, its inward momentum causes a submerged jet to form downstream. This jet narrows to a smaller cross-section than the orifice itself, referred to as the vena contracta, which is the jet's narrowest point. Surrounding this jet is a larger recirculation zone. A downstream pressure tapping, positioned beyond the orifice, detects the pressure in the vena contracta through this recirculation zone. Further, downstream, the flow undergoes diffusion, accompanied by significant total pressure loss. The introduction should be typed in Times New Roman with font size 10. Author can select Normal style setting from Styles of this template. The simplest way is to replace (copy-paste) the content with your own material. In this section, highlight the importance of topic, making general statements about the topic and presenting an overview on current research on the subject. Your introduction should clearly identify the subject area of interest.

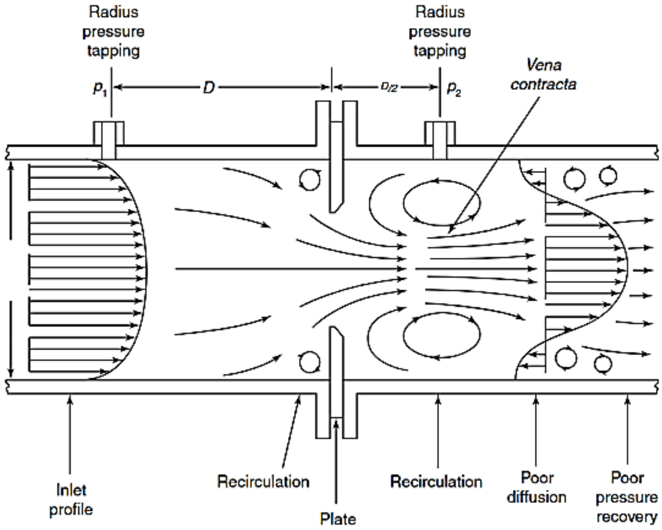

Figure 1: Geometry and flow patterns around the orifice plate flowmeter [1]

The published works in current literate conducts experimental studies to evaluate how the beta ratio (β) and Reynolds number (Re) affects the discharge coefficient (C_d) of orifice flowmeters. Using a closed-loop pipe system with adjustable orifice plates. Results showed a positive linear relationship between Cd and β, and a curvilinear relationship between (C_d) and (Re) [2, 3, 4, 5, 6].

Computational Fluid Dynamics (CFD) modelling is used for studying various aspects of orifice-plate performance and presents comparisons between CFD predictions and test data from experimental validations, Barton, N., et al [7], achieved by numerically modelling the fluid flow through the plate.

Understanding the flow dynamics through the orifice plate are required under different conditions, Abed, N., et al. [8], examined turbulent airflow through a small circular hole plate using CFD simulations in ANSYS Fluent, the study parameterized the effects of Reynolds number and the ratio of hole diameter to pipe diameter.

ANSYS Fluent also was used in Düz, H. [9], to model Conical Entrance Orifice Meters (CEOMs) with varying cone angles and beta ratios under turbulent, steady state, and incompressible flow conditions.

While Singha, R. K., et al. [10], analyzed the performance of orifice plate assemblies under non-standard conditions using CFD. The study investigated the impact of plate thickness and diameter ratio on the discharge coefficient (C_d) and the pressure loss coefficient (CL).

Filardi, M., et al. [11], conducted an evaluation on how the geometry of orifice plates influence the discharge coefficient (C_d) using Polyvinyl chloride (PVC) pipes with varying orifice diameters and edge geometries.

Therefore, Computational Fluid Dynamics (CFD) analyses play a vital role in the design, operation, and safety of crucial devices, such as orifice plate flowmeters, within nuclear reactor cooling systems. Mohamed, S. B., et al. [12] developed a mathematical model based on Bernoulli's equations, which was calibrated to achieve a specific target flow rate. Their research successfully identified the optimal beta ratio (β), ensuring the design met the required flow rate and pressure drop criteria under varying operational conditions. The findings revealed that an orifice plate design with a specific beta ratio (β) emerged as the optimal configuration for this application.
Thus, in this study, a numerical model of the orifice plate meter, originally developed by Manu, B., et al. [13], is rebuild for the purpose of conducting a wide investigation of the flow characteristics within the orifice plate meter under varying conditions, including different geometry, materials, and fluid types, using the commercial CFD software, ANSYS.

Material and methods

The methodology involves building a two-dimensional (2D) numerical model, which begins with defining the geometry of the system, followed by the creation of a computational mesh to enable accurate simulations. The two-dimensional (2D) axisymmetric simulation is an efficient and time-saving computational fluid dynamics (CFD) technique when the flow is axisymmetric. In other words, for axisymmetric or symmetric flow, 2D simplifies the problem by reducing computational complexity while still capturing the dominant flow physics which are the essential flow characteristics like velocity distribution and pressure drop. It is worth mentioning that in the upstream of the orifice plate, the flow is likely axisymmetric while it is approximately axisymmetric through the orifice[14],. The model is validated by comparing results with established experimental data. Steady-state modeling is employed to analyze the pressure and velocity fields within the orifice plate setup. Subsequently, the performance of the orifice plate is calculated based on these results. This process is repeated for different scenarios by varying parameters: the beta ratio (β), the pipe material (accounting for roughness), and the type of fluid.
Beta Ratio (β) expressed as a decimal value ranging between 0.42–0.58 to ensure sufficient pressure differential for accurate flow measurement, control of flow separation, compatibility with empirical discharge coefficient correlations validated in this range. Referencing ISO 5167 [15], which recommends (β) ratios between 0.2–0.75 for orifice plates, lower (β) values cause excessive pressure loss, while higher (β) values reduce sensitivity.
Model SST k-ω use roughness to replicate turbulent boundary layer behavior hence the SST k-ω model can be used as a Low-Re turbulence model without any extra damping functions. The roughness values represent low roughness of a well-maintained system or that of a cast iron, medium roughness simulates scaling in water pipelines, and high roughness of an untreated concrete or a severely eroded pipeline.
Arises from its compressibility and fluid-specific adjustments, whereas liquids exhibit stronger β sensitivity due to their incompressible
As illustrated in Figure 2, the integral orifice plate consists of three zones. The geometry is modeled with an orifice diameter (d) of 25 mm, a pipe diameter (D) of 50 mm, a beta ratio (β) of 0.5, and a plate thickness (t) of 2.5 mm. The upstream and downstream sections are extended for lengths of 10D=500 mm and 15D=750 mm, respectively, as per the model parameters specified by the referenced study [13].

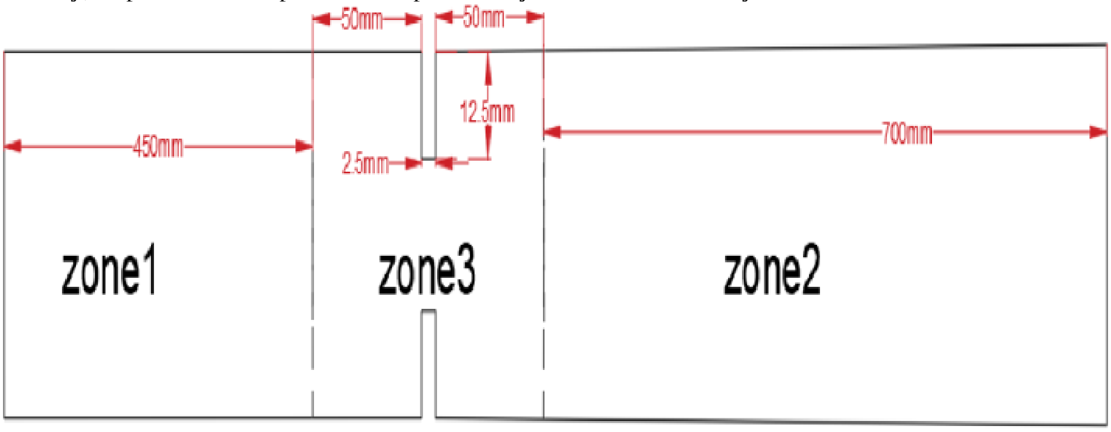

Figure 2: Computer-aided design of an integral orifice plate consists of three zones.

The accuracy and computational efficiency of the 2D simulations rely on the resolution of the computational grid. A two-dimensional mesh is employed, featuring a dropped mesh configuration to accommodate midsize nodes of the orifice plate geometry. The size function is set to proximity, with coarse relevance center and medium smoothing applied. The minimum edge length is defined as 2.5 mm. The flow domain, encompassing the integral orifice plate, is discretized into 383,861 mesh elements and 366,793 mesh nodes. An overview of the discretized flow domain is depicted in Figure 3, where a plan view is presented.

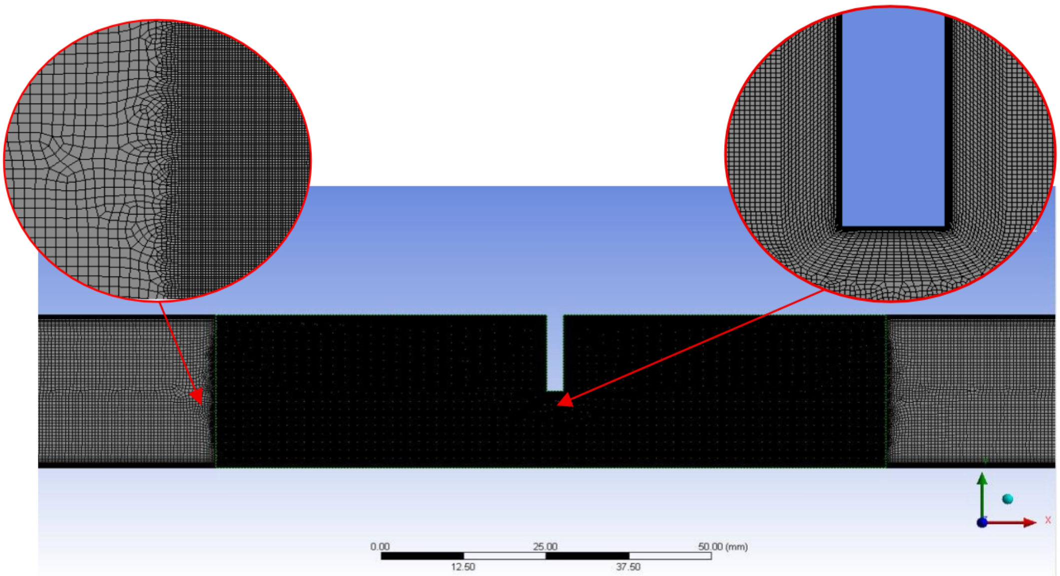

Figure 3: Two-dimensional (2D) CFD model grid in the XY plane.

Boundary conditions were defined as: a no-slip wall boundary condition, an inlet boundary condition velocity specified as a constant in the x-direction, and an outlet boundary condition as a constant to represent an open outlet allowing the fluid to exit freely without constraints. The two-equation eddy-viscosity model, shear stress transport (SST) k-ω turbulence model, is applied within the inner boundary layer suitable as a low-reynolds turbulence model without requiring additional damping functions. Adopting a convergence criterion of 10-6, ensuring highly accurate numerical solutions. Using a turbulence model and flange pressure tapings, the differential pressure is measured to calculate mass flow rate, density, and the geometrical properties of the orifice meter,

The flow through the standard square-edged orifice plate was analyzed, and the results were compared to the standard values specified in ISO 5167 [15]. The numerical model was validated against experimental data [15]; Figure 4 shows a maximum error of 8.11% and a minimum error of 2.39%.

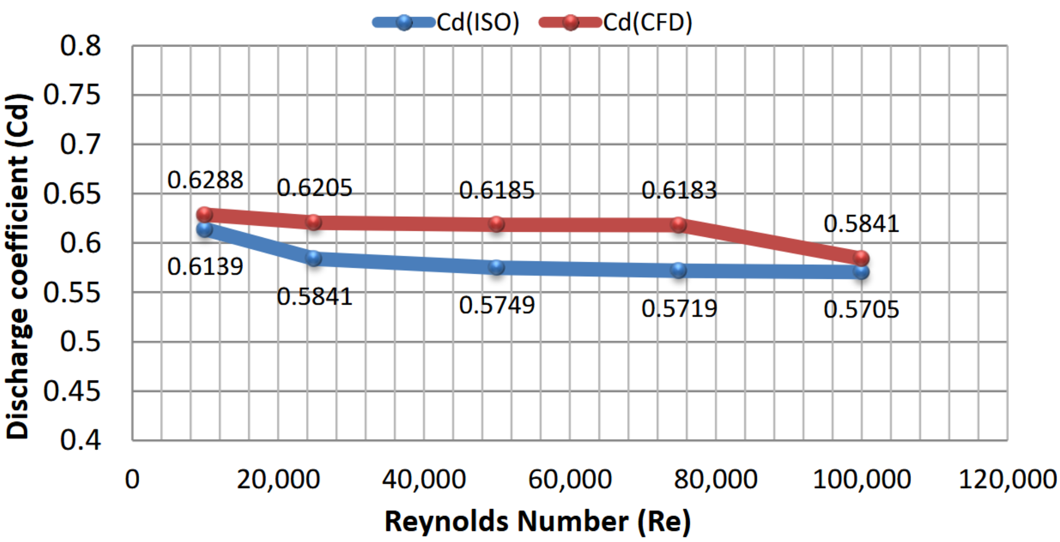

Figure 4: Discharge coefficient (C_d) variation using ISO standards and CFD simulations**.**

These errors fall within acceptable limits that establish the numerical model as reliable for the investigation [16, 17]. The coefficient of discharge (C_d) was calculated using the formula provided in ISO 5167 [15], which is based on the Reader-Harris/Gallagher equation:

$$C_d = 0.5961 + 0.0261\,\beta^2 - 0.0261\,\beta^2 + 0.000521\left(\frac{10^6\ \beta^2}{Re}\right)$$
$$+ (0.0188 + 0.0063A)\ \beta^{3.5}\left(\frac{10^5\ \beta}{Re}\right)(0.043 + 0.08\,e^{-10\,L_1}$$
$$- 0.123\,e^{-7\,L_1})(1 - 0.11\,A)\left(\frac{\beta^4}{1-\beta^4}\right) - 0.031\,(M1 - 0.08\,M11.1)\beta^{1.3}$$

The analysis focuses on examining the pressure and velocity fields for various fluids flowing at a constant inlet velocity, considering different surface roughness levels. Throughout Numerical experiments, the pipe diameter fixed at 50 mm. The study explores five orifice plate diameters: 21 mm, 23 mm, 25 mm, 27 mm, and 29 mm. Three fluid types, coded as water (density: 1000 kg/m³), air (density: 1.225 kg/m³), and oil (density: 803.5 kg/m³). In addition, three surface roughness levels as 0.08, 0.5, and 0.9.

Results and discussion

Figures 5, 6, and 7 illustrates the relationship between (β) and (C_d) for various fluids.

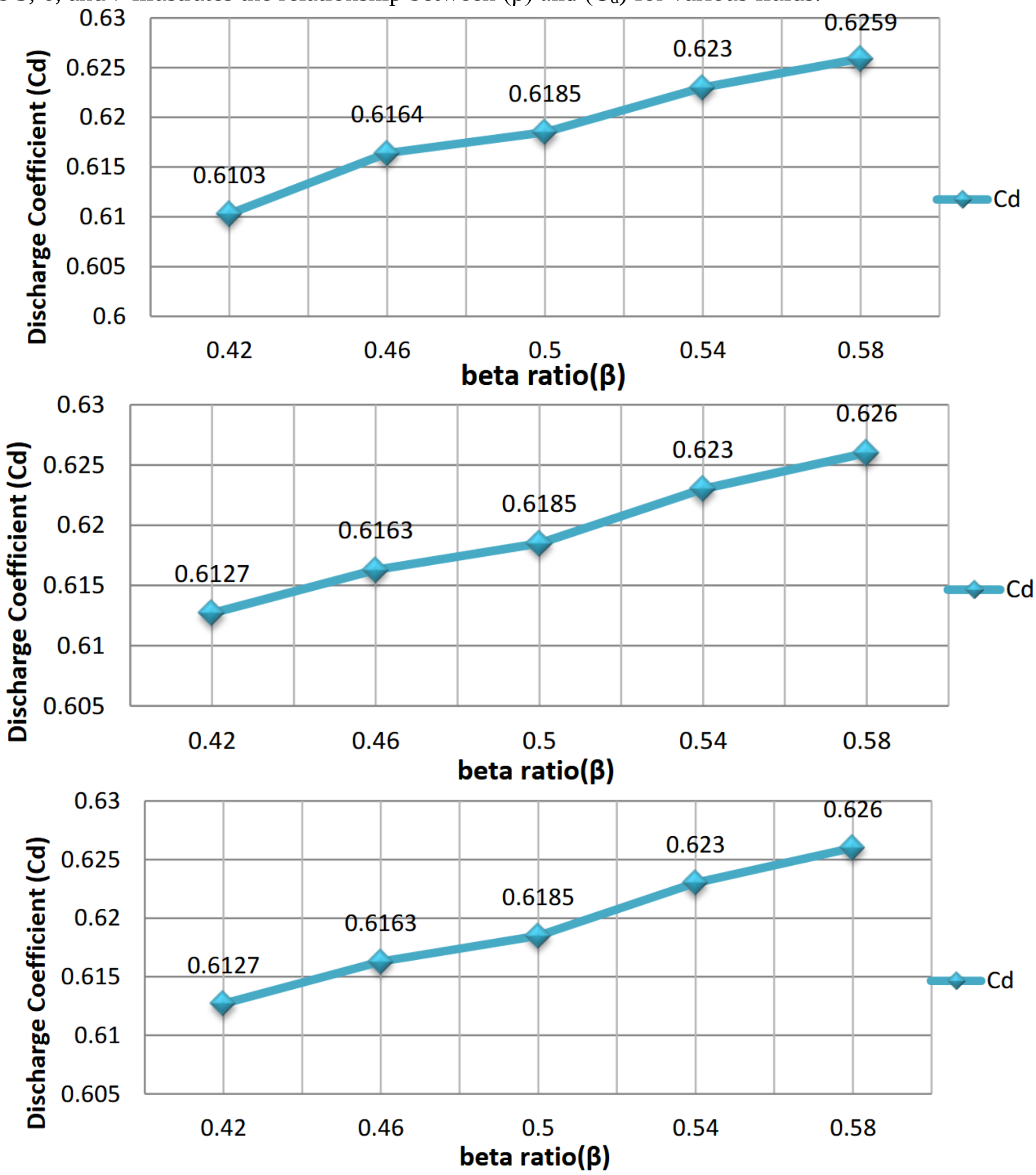

Figure 5: The discharge coefficient (Cd) as a function of beta ratio (β) for water flow at constant roughness values at (from top to bottom) 0.08, 0.5, and 0.9

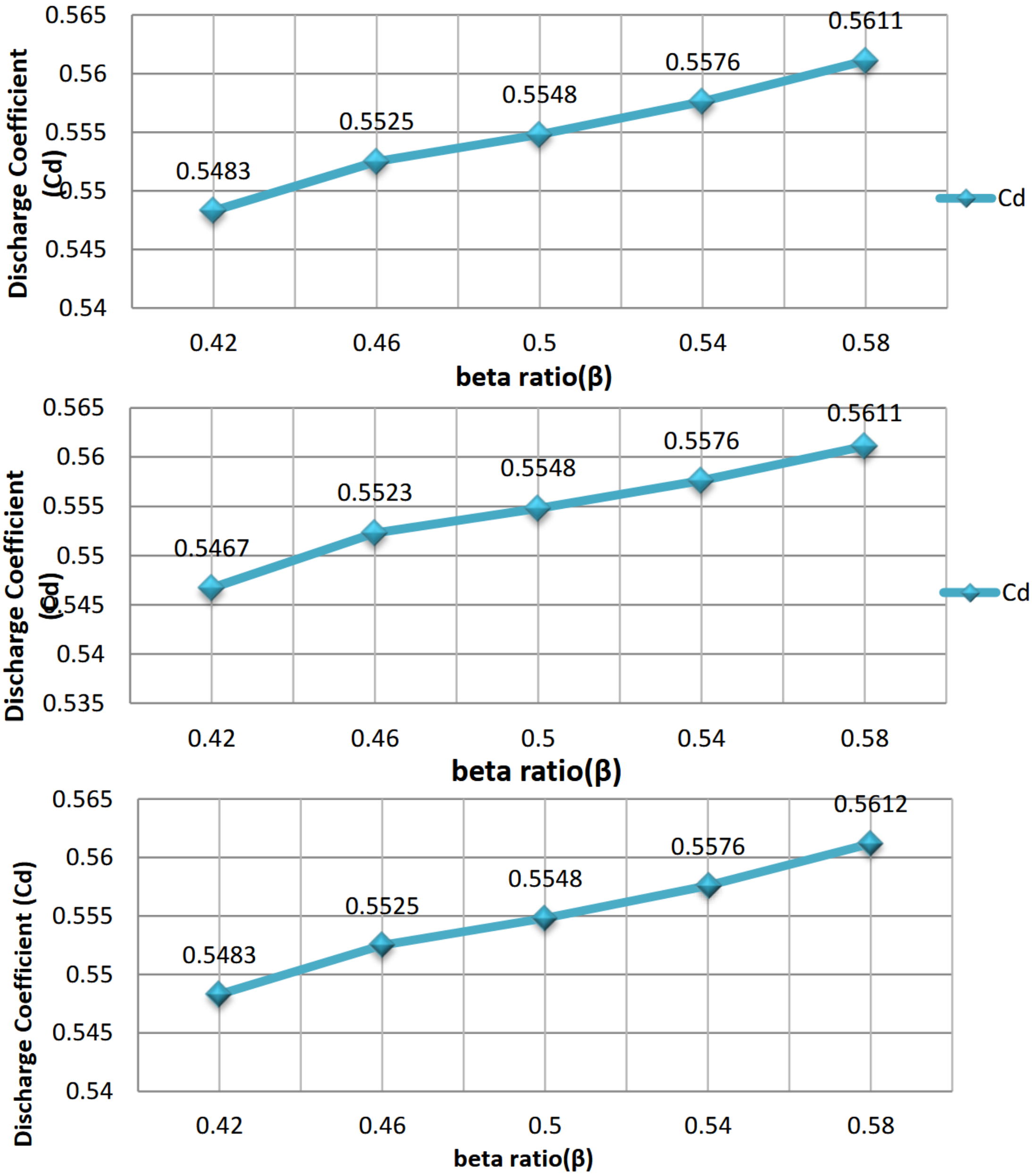

Figure 6: The discharge coefficient (Cd) as a function of beta ratio (β) for oil flow at constant roughness values at (from top to bottom) 0.08, 0.5, and 0.9

The data reveal an upward trend, with the discharge coefficient (C_d) increasing as the beta ratio (β) increases. The maximum (C_d) value of 0.58 is observed for an orifice diameter of 29 mm, corresponding to (C_d) values of 0.6393, 0.5612, and 0.0224 for water, oil, and air, respectively.
The discharge coefficient (C_d) generally increases with a higher beta ratio (β). However, unlike water and oil, the (C_d) values for air show only a slight increase with increasing beta ratios, irrespective of roughness levels. Moreover, the roughness does not significantly affect the discharge coefficient for air due to the compressibility nature of air. For water and oil, roughness has minimal impact on the discharge coefficient at a Reynolds number (Re) of 50,000. Similar results were reported by Rahman (2009) [7], and ISO 5167 [15].

The velocity profile “contour” results reveal an inverse relationship between the orifice diameter and fluid velocity. Figure 8, shows a simulation of the flow of three fluids (a) water, (b) oil, and (c) air through an orifice plate with a beta ratio of 0.42.

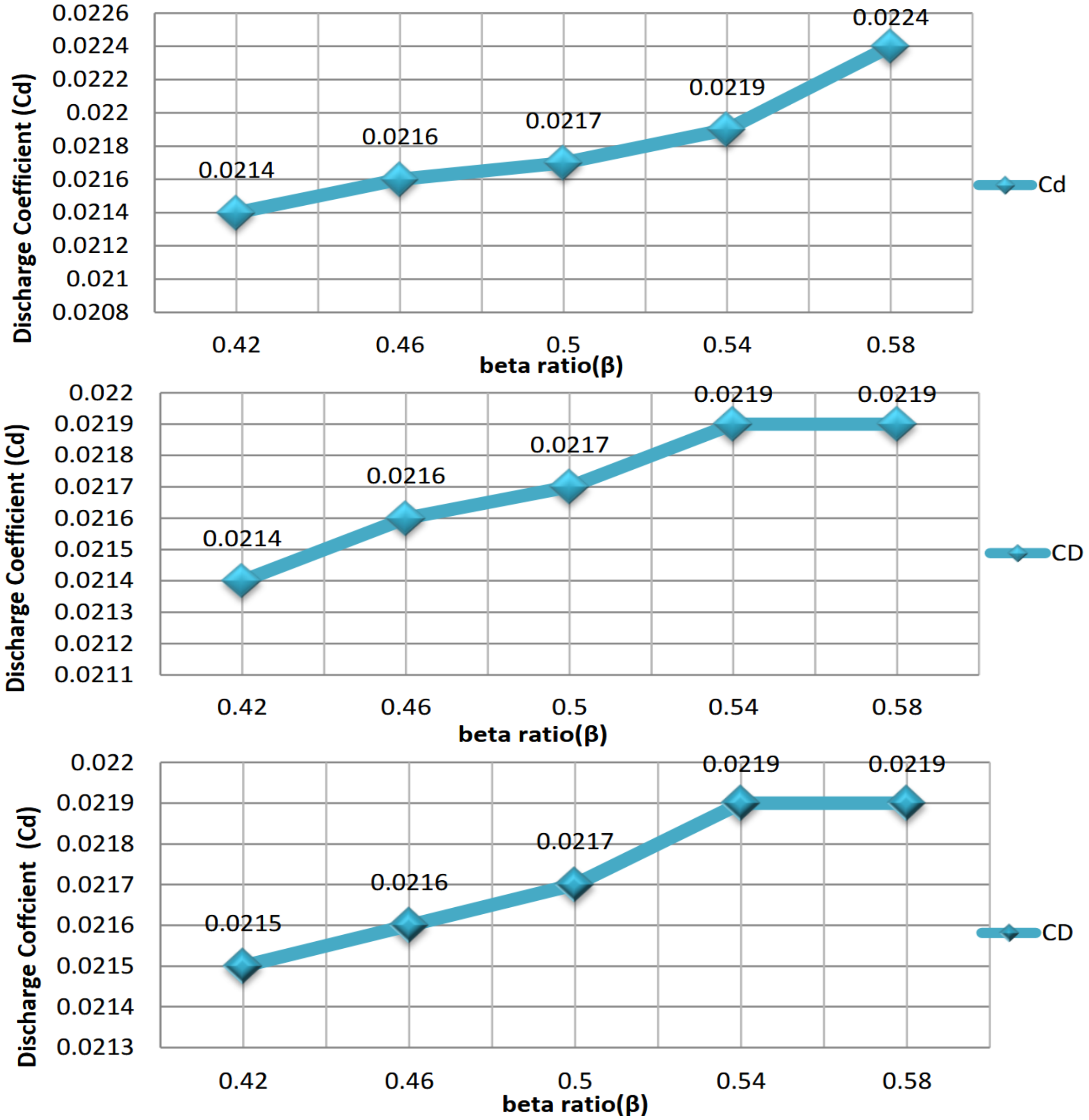

Figure 7: The discharge coefficient (Cd) as a function of beta ratio (β) for airflow at constant roughness values at (from top to bottom) 0.08, 0.5, and 0.9

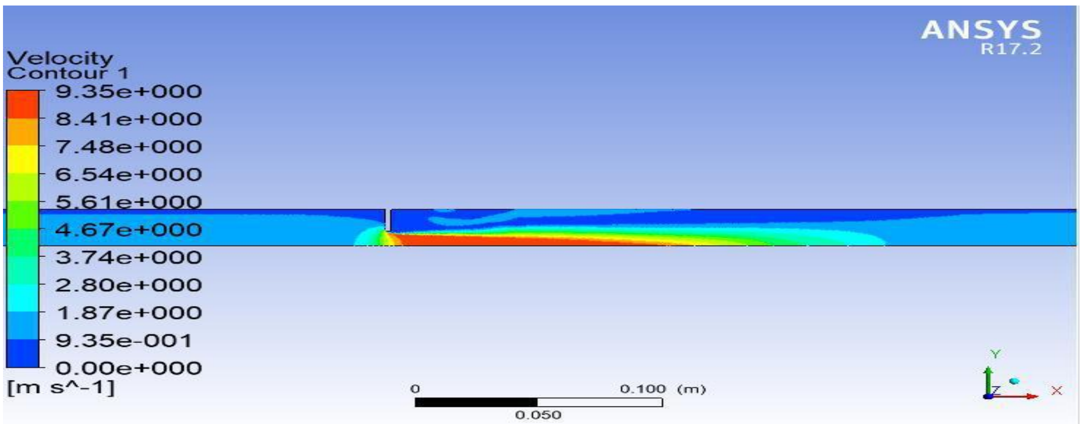

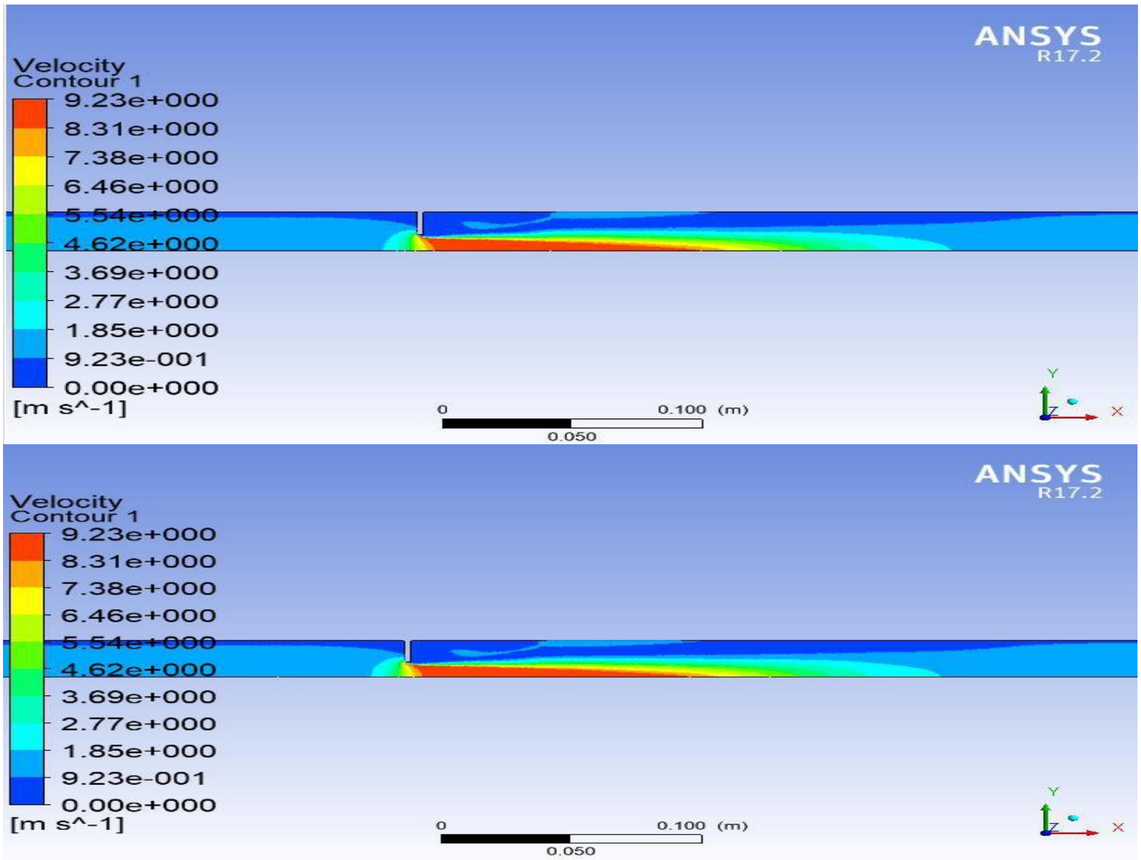

Figure 8: Velocity contours of flow at a beta ratio of $\beta = 0.42$ for (from top to bottom) water, oil, and air.

As fluids approach the constriction, the velocity increases due to a sudden rise in pressure caused by the reduced cross-sectional area. Fluids exiting the orifice exhibit a sharp velocity increase compared to the inlet. Furthermore, the velocity distribution across the pipe's cross-section is non-uniform, with the highest velocity concentrated at the center.

Water, oil, and air displayed similar velocity profiles, particularly near the orifice exit. The maximum velocities were 9.35 m/s for water, 9.23 m/s for oil, and 9.23 m/s for air. Increasing the orifice diameter resulted in a reduction in fluid flow velocity, aligning with the continuity equation. At this beta ratio, vortex formation was observed farther downstream compared to a beta ratio of 0.42, with the vortices being less pronounced, allowing the fluid to travel further and interact with the pipe walls in a more uniform manner.

An increase in the beta ratio to 0.5, as seen in Figure 9, caused the formation of vortices to be nearly eliminated, leading to a smoother fluid flow.

The maximum velocities recorded for water, oil, and air at this diameter were 6.38 m/s, 6.37 m/s, and 6.37 m/s respectively. The velocity profiles of water, oil, and air exhibit similar patterns, particularly near the orifice exit.

Increasing the flow area, Figure 10, to a beta ratio of 0.58 led to greater variations in fluid velocity, with the fluids traveling a shorter distance compared to smaller beta ratios. The velocity gradient across the flow field also became less pronounced. This is evident in the case of water, where the maximum velocity was recorded at 9.35 m/s for an orifice diameter of 21 mm. As the orifice diameter increased, the velocity gradually decreased, reaching the lowest value of 4.63 m/s at an orifice diameter of 29 mm.

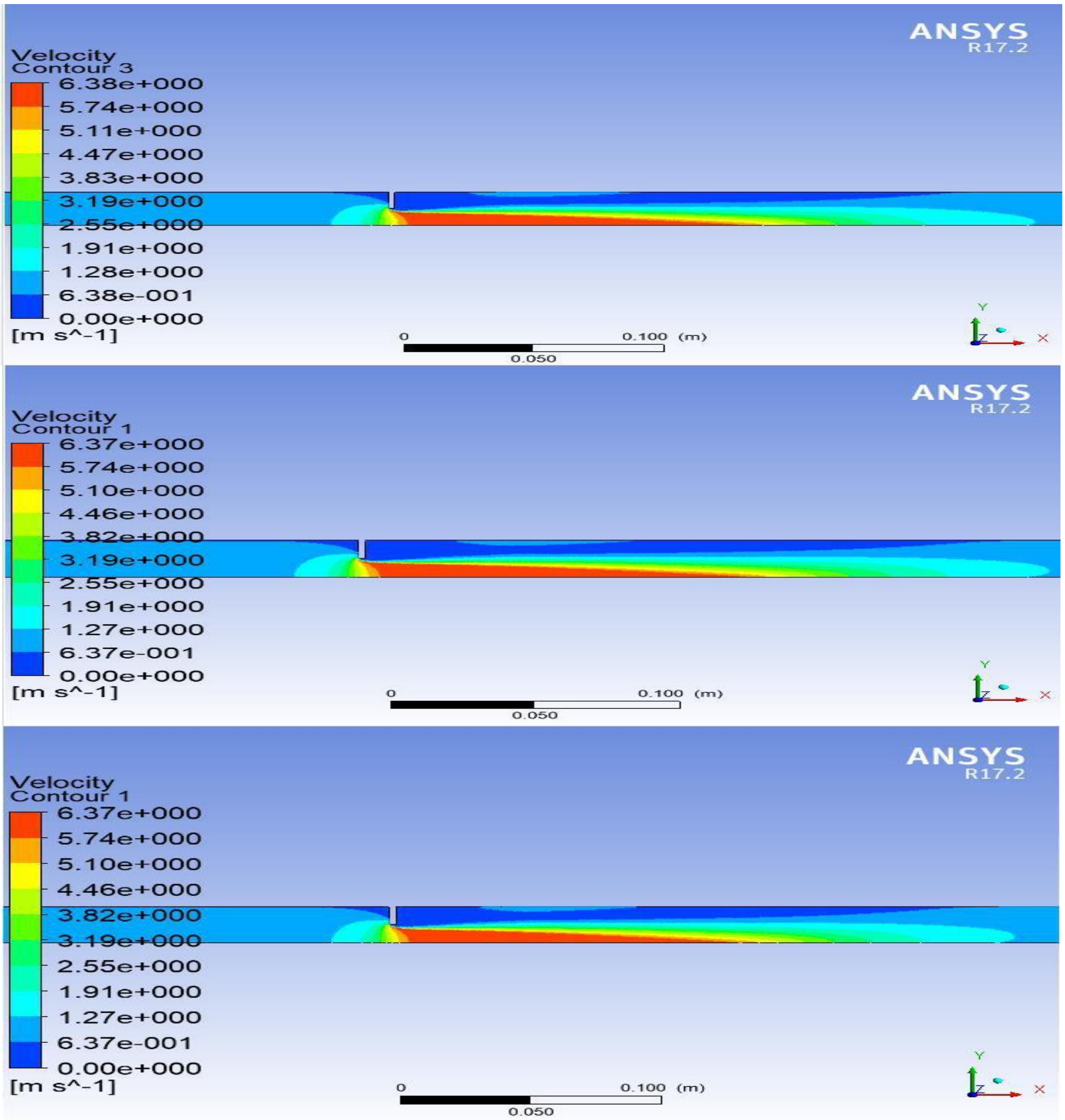

Figure 9: Velocity contours of flow at a beta ratio of β = 0.5 for (from top to bottom) water, oil, and air

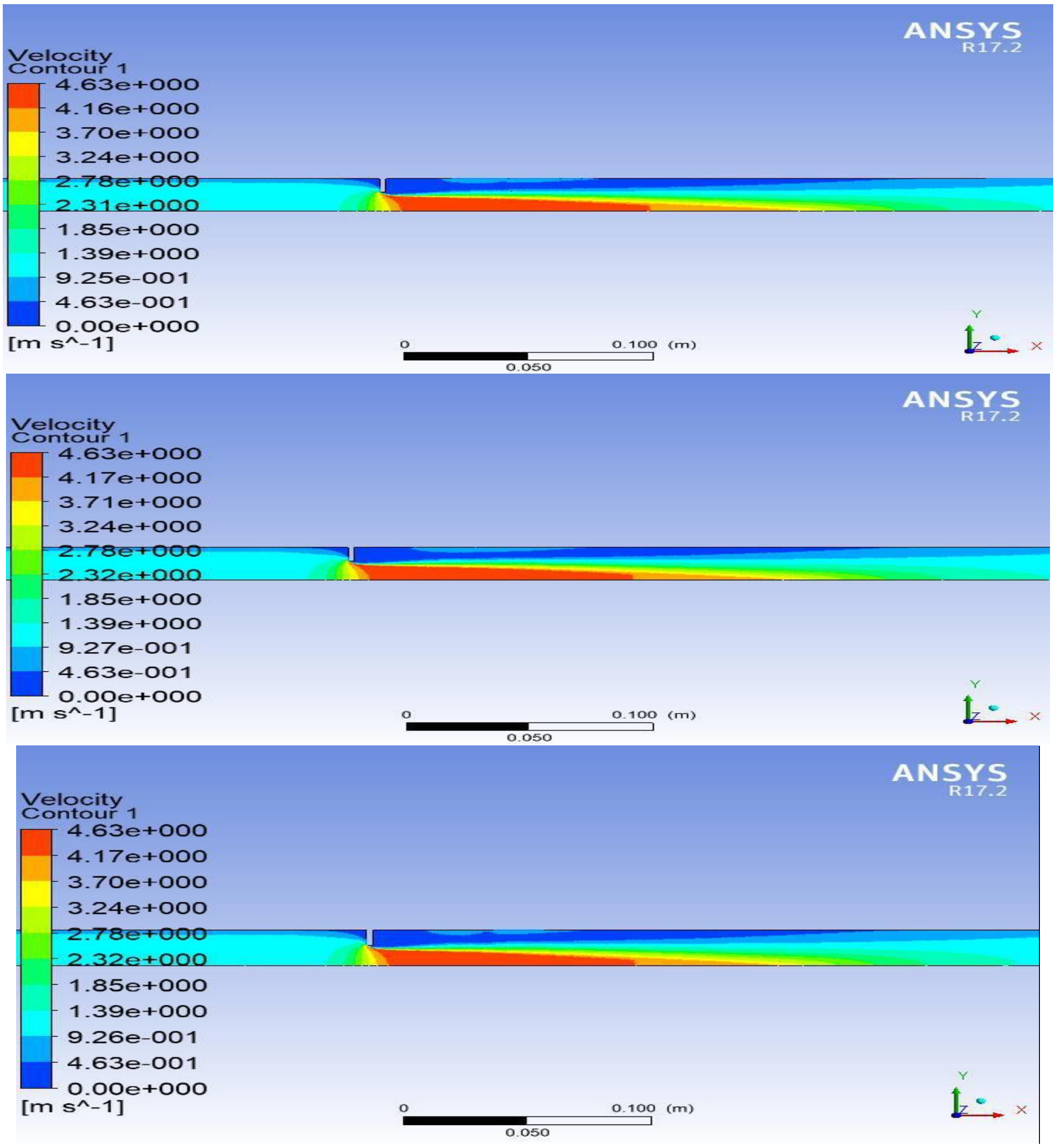

Figure 10: Velocity contours of flow at a beta ratio of $\beta = 0.58$ for (from top to bottom) water, oil, and air.

It was observed that the fluid velocity decreases as the diameter of the orifice increases-an inverse relationship between orifice diameter and velocity.

The velocity profiles for water, oil, and air appear to converge at the extremes of the diameter range, indicating that the velocity differences between water, oil, and air diminish at the smallest and largest measured diameters.

Pressure lines, Figure 11, illustrate the distribution of pressure within a fluid system. A significant pressure drop occurs between the inlet and outlet of the orifice, due to the Bernoulli principle. As the fluid accelerates through the constricted cross-sectional area of the orifice, its pressure decreases.

Increasing the beta ratio results in a greater pressure drop at the orifice outlet. This occurs because a reduction in the cross-sectional area of the inlet leads to an increase in fluid velocity.

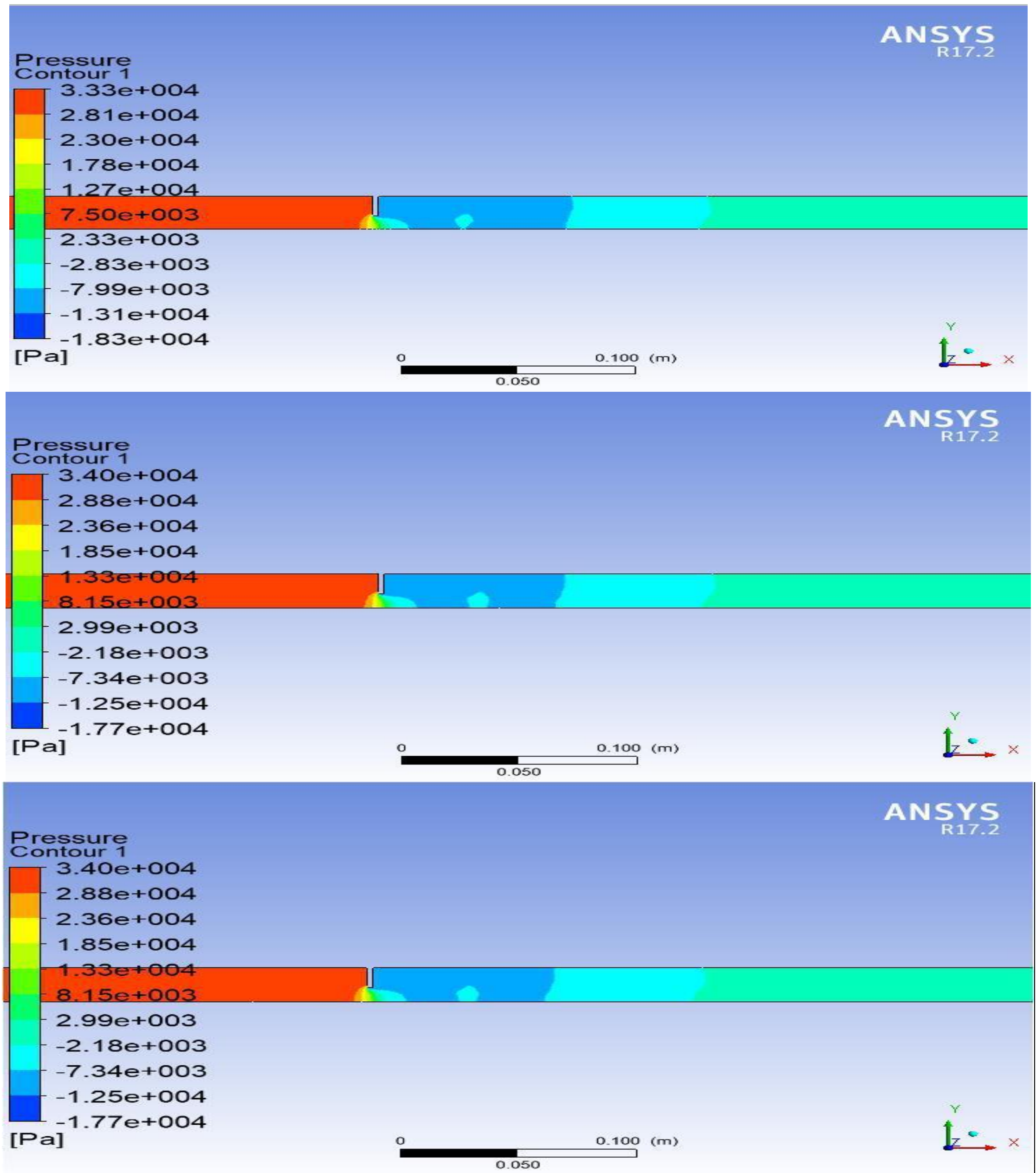

Figure 11: Pressure contours of flow at a beta ratio of β = 0.42 for (from top to bottom) water, oil, and air.

Throughout the flow path, Figure 12, the highest pressure is observed at the orifice inlet, while the lowest pressure occurs at the throat—the narrowest section of the orifice. As the fluid passes through the throat, it accelerates, resulting in a pressure drop. Beyond the throat, the flow path widens, causing the fluid velocity to decrease and the pressure to gradually rise until it stabilizes at the outlet.

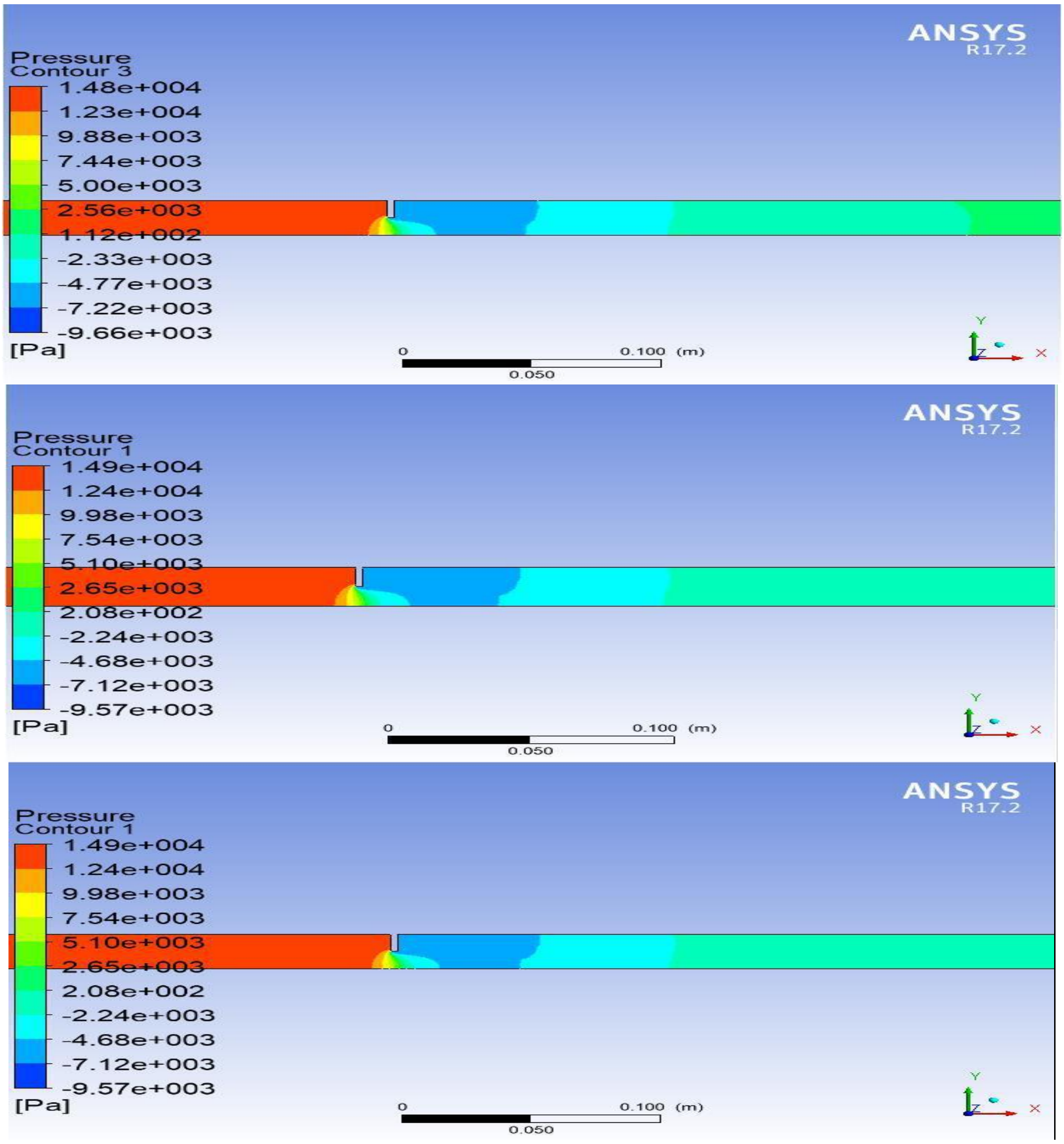

Figure 12: Pressure contours of flow at a beta ratio of $\beta = 0.5$ for (from top to bottom) water, oil, and air.

Narrowing the throat opening results in a higher fluid velocity and a greater pressure drop. However, with an increased beta ratio, the orifice contraction becomes less severe, leading to a less abrupt change in velocity and a smoother pressure gradient. As beta increases, the pressure drop becomes less influenced by changes in inlet velocity. Additionally, the pressure distribution within the tube transitions from being concentrated to exhibiting a more dispersed pattern. Figure 13 illustrates the flow through the orifice plate at a beta ratio of 0.58. In this part of study the incompressible flow through integral orifice plate assemblies is simulated or analyzed and results are compared with the experimental results reported in the literature. For this purpose, the experimental data reported in ISO 5167 [15].

Numerical experiments revealed that increasing the beta ratio of an orifice plate to 0.58—the highest value tested—resulted in a more even pressure distribution across the plate, rather than concentrating it at a single point. This phenomenon occurs due to the larger throat diameter associated with higher beta ratios, which reduces flow restriction. As a result, the pressure drop (ΔP) at the plate outlet decreases. Consequently, the pressure gradient along the flow path ($\partial P/\partial x$) becomes less pronounced, leading to a more uniform pressure distribution throughout the pipe. These research findings are supported by ISO 5167 [15] experimental data.

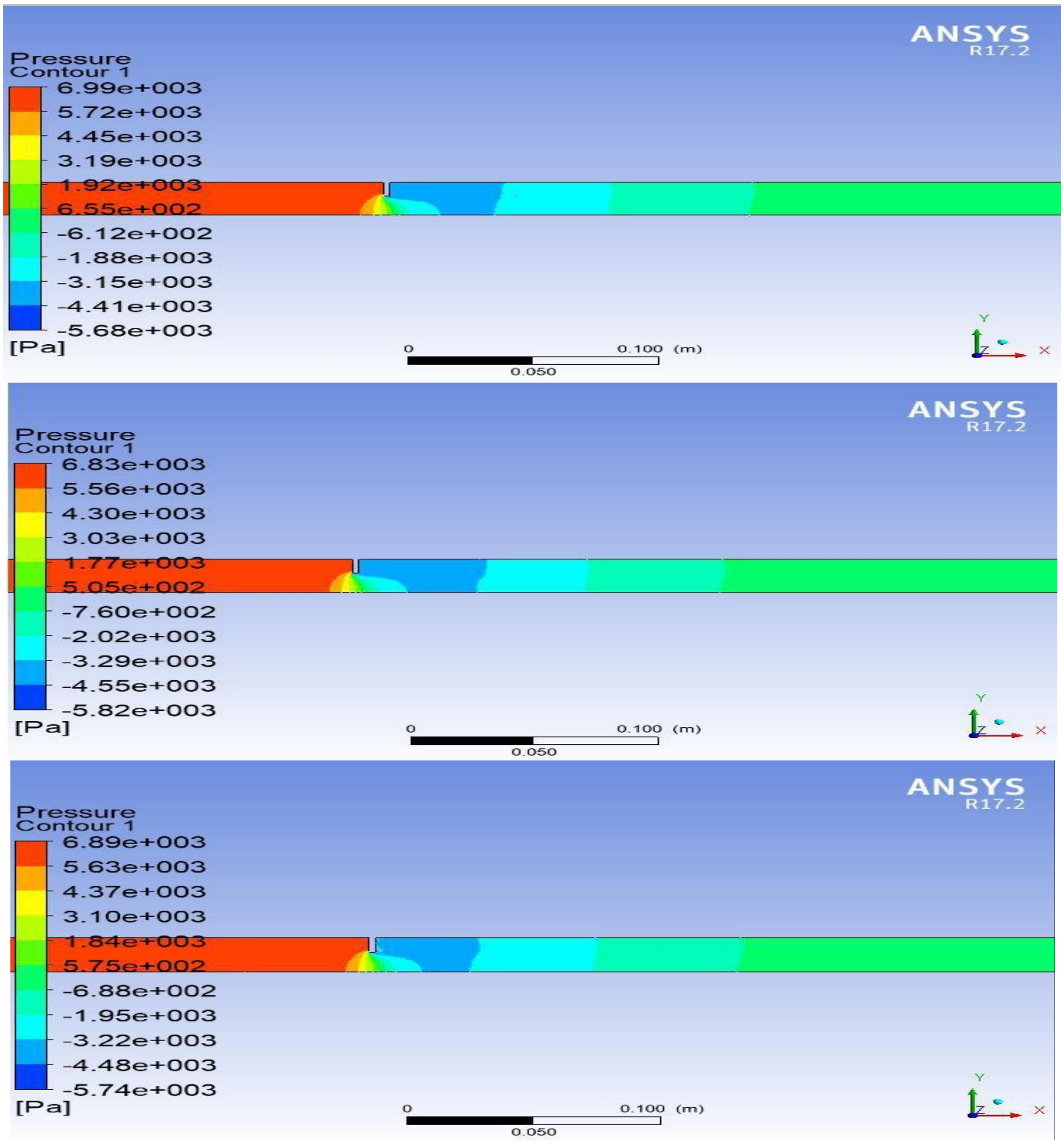

Figure 13: Pressure contours of flow at a beta ratio of $\beta = 0.58$ for (from top to bottom) water, oil, and air

Conclusion

In conclusion, the numerical experiments demonstrated that an increase in orifice diameter and beta ratio leads to a decrease in fluid pressure and an increase in the discharge coefficient (C_d). For all three tested fluids-water, oil, and air-this trend was consistently observed. The highest-pressure values were recorded at the smallest orifice diameter of 21 mm, with 3.33×10^4 Pa for water and 3.4×10^4 Pa for oil and air. The pressure decreased steadily as the orifice diameter increased, reaching the lowest values of 6.99×10^3 Pa for water and 6.83×10^3 Pa for oil and air at a diameter of 29 mm.

The discharge coefficient (C_d) increased with the beta ratio for all three fluids, with the most pronounced trend observed in water, where (C_d) rose from approximately 0.61 at a beta ratio of 0.42 to around 0.64 at a beta ratio of 0.58. Surface roughness had minimal impact on (C_d), these findings optimize orifice meter design by demonstrating that increasing the beta ratio (β)—achieved through a larger orifice diameter relative to the pipe diameter—enhances the discharge coefficient (C_d), improving flow measurement accuracy, while velocity profiles for the fluids displayed similar characteristics near the orifice exit. The results also revealed an inverse relationship between orifice diameter and fluid velocity, as well as between velocity and pressure. Furthermore, a lower beta ratio resulted in a greater pressure drop, minimizing the orifice meter pressure loss, by choosing optimal beta ratio, reduces the energy consumption of industrial facilities and pipelines.

Overall, the study highlighted the dependence of discharge coefficient (C_d), velocity range, and pressure range on the beta ratio (β) for all three fluids, providing valuable insights into flow behaviour through orifice plates under varying conditions.

Future work will involve expanding parametric analyses to broader Reynolds numbers, roughness values, beta ratios, and diverse fluids, external temperature effects on fluid viscosity and flow to further extend the investigation. Transitioning to 3D simulations would improve flow visualization and measurement for real-world case studies, affecting fluid dynamics research.

References

[1] Baker, R. C. (2016). *Flow Measurement Handbook: Industrial Designs, Operating Principles, Performance, and Applications*. Cambridge University Press.

[2] Almutairi, J. H., Pašić, M., Džaferović, E., & Hasečić, A. (2025). Prediction of discharge coefficients for contaminated circular multi-hole orifice flow meters with deep learning algorithms. *Physics of Fluids*, *37*(2). https://doi.org/10.1063/5.0252899

[3] Parshad, H., & Kumar, R. (2024). Effect of Varying Diameter of Orifice on Coefficient of Discharge. *International journal of engineering sciences paradigms and researches*.

[4] Assran, M. H., shenouda, B., & Mohamed, H. I. (2022). *Effect of Orifice-Meter Shape on Discharge Coefficient and Head Loss through It*. https://doi.org/10.21203/rs.3.rs-1741688/v1

[5] Ridlah, M. R. (2022). Experimental and numerical study of basic discharge coefficient (CD) for orifice plate meters under single phase fluid flow. *Proceedings of Indonesian Petroleum Association, 46th Annual Convention & Exhibition, 2022*. https://doi.org/10.29118/ipa22-f-4

[6] Barton, N., Reader-Harris, M., & Gibson, J. (2004). Overview of CFD modelling of orifice-plate flowmeters. In Proceedings of the North Sea Flow Measurement Workshop (pp. 1-16).

[7] Rahman, M., Biswas, R., & Mahfuz, W. (2009). Effects of beta ratio and Reynold's number on coefficient of discharge of orifice meter. *Journal of Agriculture & Rural Development*, 151–156. https://doi.org/10.3329/jard.v7i1.4436

[8] Abed, N., Hassan, H. F., Al-Damook, A., & Khalil, W. H. (2020). Experimental and numerical investigations for turbulent air flow characteristics of circular orifice plate. *IOP Conference Series: Materials Science and Engineering*, *881*(1), 012050. https://doi.org/10.1088/1757-899x/881/1/012050

[9] Düz, H. (2021). Effect of conical angle on the hydraulic properties of orifice plate flows: A numerical approach. *Flow Measurement and Instrumentation*, *81*, 102026. https://doi.org/10.1016/j.flowmeasinst.2021.102026

[10] Singh, R. K., Singh, S. N., Seshadri, V. (2010). Performance evaluation of orifice plate assemblies under non-standard conditions using CFD. *Indian Journal of Engineering & Materials Sciences*, 17, 397-406.

[11] Filardi, M., Vieira, E. D. R., & Mansur, S. S. (2012). Experimental flow measurement with integral orifice. *14th Brazilian Congress of Thermal Sciences and Engineering*.

[12] Mohamed, S. B., Mansour, M. S., & Dekam, E. I. (2019). A 5-30 kg/s Orifice Plate Cooling Water Flow Meter Design, *International Journal of Recent Development in Engineering and Technology, volume 8, Issue 2*

[13] Manu, B. V., Kumar, K. J., & Seshadri, V. (2019). CFD Analysis of Flow through Integral Orifice Plate Assemblies under Diverse Working Conditions. *International Research Journal of Engineering and Technology (IRJET), volume 6, Issue 6,* 1699-1705.M. Young, The Technical Writer's Handbook. Mill Valley, CA: University Science, 1989.

[14] Rahul Krishna, H., Issac, M. T., & Ebenezer, D. D. (2023). Numerical investigation of two-dimensional axisymmetric and three-dimensional flow simulations over a benchmark underwater vehicle. *Physics of Fluids*, *35*(1).

[15] International Organization for Standardization. (2003). *Measurement of fluid flow by means of pressure differential devices inserted in circular cross-section conduits running full—Part 1: General principles and requirements* (ISO Standard No. 5167-1:2003). https://www.iso.org/standard/30090.html

[16] Hamza, E. (2020). Dimensions Effect of the Rotating Fluid Zone on the Results when CFD Modeling of Friction Stir Welding. *Third Conference for Engineering Sciences and Technology* (CEST-2020). 01-03 December 2020 /Alkhoms – Libya

[17] Hamza, E. (2021). Cfd-modelling and thermal characterization of friction stir welding using tool with polygonal pins. *J Eng Res*, *32*, 43-78.